THERMAL MANAGEMENT OF LITHIUM-ION BATTERY PACK USING AIR COOLING METHOD

THESIS SUBMITTED IN PARTIAL FULFILMENTS OF THE REQUIREMENT FOR THE DEGREE OF MASTER OF ENGINEERING IN MECHANICAL ENGINEERING UNDER FACULTY OF ENGINEERING AND TECHNOLOGY

Submitted by

SURANJAN KHATUA
Class Roll Number: 002011204013
Academic Session: 2020-2022
Exam Roll No.: M4AUT22013

Under the guidance of
Prof Sourav Sarkar
Department of Mechanical Engineering
Jadavpur University

DEPARTMENT OF MECHANICAL ENGINEERING

JADAVPUR UNIVERSITY

188, RAJA S.C. MULLICK ROAD, KOLKATA- 700032

DECLARATION OF ORIGINALITY AND COMPLIANCE OF ACADEMIC ETHICS

I, hereby declare that the thesis entitled **"THERMAL MANAGEMENT OF LITHIUM-ION BATTERY PACK USING AIR COOLING METHOD"** contains literature survey and original research work by the undersigned candidate, as a part of his MASTER OF ENGINEERING IN AUTOMOBILE ENGINEERING under the Department of Mechanical Engineering, studies during academic session 2020-2022.

All information in this document have been obtained and presented in accordance with academic rules and ethical conduct.

I also declare that, as required by these rules of conduct, I have fully cited and referenced all material and results that are not original to this work.

Name: **SURANJAN KHATUA**

Class Roll Number: **002011204013**

Examination Roll Number: **M4AUT22013**

Date:

Signature:

FACULTY OF ENGINEERING & TECHNOLOGY
DEPARTMENT OF MECHANICAL ENGINEERING
JADAVPUR UNIVERSITY, KOLKATA

CERTIFICATE OF RECOMMENDATION

.

This is to certify that the thesis entitled "**Thermal Management of Lithium-Ion Battery Pack Using Air Cooling Method**" is an authentic work carried out by SURANJAN KHATUA under our supervision and guidance in partial fulfilment of the requirements for awarding the degree of Master of Engineering in Automobile Engineering under Department of Mechanical Engineering, Jadavpur University during the academic session 2020-2022.

THESIS SUPERVISOR
Prof. Sourav Sarkar
Assistant Professor
Department of Mechanical Engineering
Jadavpur University, Kolkata

Prof. (Dr.) Chandan Mazumdar
Dean

Faculty Council of Engineering and Technology
Jadavpur University, Kolkata

Prof. (Dr.) Amit Karmakar
Head of Department

Department of Mechanical Engineering
Jadavpur University, Kolkata

FACULTY OF ENGINEERING & TECHNOLOGY
DEPARTMENT OF MECHANICAL ENGINEERING
JADAVPUR UNIVERSITY
KOLKATA-700032

CERTIFICATE OF APPROVAL

The foregoing thesis, entitled "**THERMAL MANAGEMENT OF LITHIUM ION BATTERY USING AIR COOLING METHOD**" is hereby approved as a creditable study in the area of Automobile Engineering carried out and presented by SURANJAN KHATUA in a satisfactory manner to warrant its acceptance as a prerequisite to the degree for which it has been submitted. It is notified to be understood that by this approval, the undersigned do not necessarily endorse or approve any statement made, opinion expressed and conclusion drawn therein but approve the thesis only for the purpose for which it has been submitted.

Committee of final evaluation of Thesis

_____

_____

_____

_____

_____

_____

Signature of Examiners

ACKNOWLEDGEMENT

I would like to record here my gratitude to all who supported me and gave constructive suggestions during the completion of this paper.

Separately, I express my deepest gratitude to **Prof. Sourav Sarkar Sir**, Assistant Professor, Department of Mechanical Engineering for his invaluable guidance. The regular discussions and idea-sharing with my thesis supervisors really helped me to improve my knowledge day by day my research related problems. At the beginning of this work, they gave me the valuable instruction that properly guided me in right path to accomplish this paper. It was really a pleasure work under their supervision.

I sincerely believe that I was fortunate enough to have come across **Prof. Sourav Sarkar Sir**, who can inspire someone to work wonders. It would really have been not possible for me to complete this thesis without his assistance, proper guidance and motivation. He always helped me during the critical phase of this thesis and was always available for me for any query, whether it's a telephonic or a face-to-face discussion. Above all he enhanced my confidence and guided me throughout my work.

I thank my batch mates and seniors for their consistent support throughout. In this regard I tender special thanks to **Mr Saumendra Nath Mishra** PhD scholars, for giving me valuable suggestions and allowing me to access their systems whenever needed.

I am highly indebted to all my professors, their guidance and supervision as well as for providing necessary information regarding thesis and also for their support in completing my master's thesis.

I would like to express my gratitude towards my parents and my younger brother for their kind cooperation and encouragement which helped me in the completion of my master's thesis.

Finally, my thanks and appreciations also go to my dear friends in developing my master's project and people who have willingly helped me out with their abilities.

Suranjan Khatua

M.E (Automobile Engineering)

2nd Year, Final Semester

Department of Mechanical Engineering

Jadavpur University, Kolkata

LIST OF CONTENTS

List of figures and tables

Table

Nomenclature

Li pf6	Lithium hexafluorophosphate
LIB	Lithium Ion Battery
BTMS	Battery Thermal Management System
B.E.V	Battery Electric Vehicle
H.E.V	Hybrid Electric Vehicle
R134a	1,1,1,2-Tetrafluoroethane
R1234yf	2,3,3,3-Tetrafluoropropene
ISC.	Internal Short Circuit
P.C.M	Phase Change Material
EV	Electric Vehicles
F.V.M	Finite Volume Method
N.T.U.	Number of transfer units
CFD	Computational Fluid Dynamics
PCM	Phase Changing Material
V	Volume
P	Density
C	Specific Heat of body zone
T	Temperature
K	Thermal conductivity of battery

P	Density
M	viscosity of fluid
F	Body Force
E	Total energy of fluid zone
$\mathbf{K_f}$	thermal conductivity of fluid
K	Kelvin

CHAPTER-1

INTRODUCTION

1.1 Thermal Management of Electric Vehicle

Internal combustion (IC) engines are used in the majority of the cars we encounter on a daily basis. Most of us think that an electric vehicle works on battery pack or electricity but there are three types of electric vehicles to know about. First one is Battery Electric Vehicle (B.E.V.). B.E.V are fully electric which means they are powered by battery packs and electricity and the batteries might be lithium ion batteries(LIB), lead acid batteries and ultra-capacitor as well(Tata Electric car, Nissan Leaf etc).There is no fuel tank, only charger available in these types of vehicles. Hybrid Electric Vehicle (H.E.V) is a combination of both internal combustion engine and electric motor. Here electric vehicle work with both petrol and batteries. Batteries are charged during braking and the mechanism is called regenerative braking system. Final one is plug-in Hybrid Electric Vehicle. They powered by both petrol and electricity, in this type batteries get recharged with 'Plugging-in' supply and as well as regenerative braking system.

It will surprise us to learn that electric cars predate the twenty-first century. In other words, electric motors debuted about at the same time as petroleum-powered engines (that is, the ones that run on fossil fuels like gas and diesel). The first electric motor prototype was created in 1828 by a Hungarian engineer named "Anyos Jedik," who used it to power a toy automobile at the time. Even though a battery-powered car was supposed to revolutionize how people lived their lives. In light of this, electric vehicles are causing quite a stir in the automotive industry. By 2025, electric vehicles are anticipated to outnumber conventional internal combustion vehicles.

As a result, it is obvious that a battery is necessary for any electric vehicle. Where there is a battery, heat creation is possible; if the heat is not removed, there is a considerable risk of damage.

1.2 Description of Lithium ion Battery:

The world is currently experiencing an electric revolution, which has increased demand for more affordable, smaller, and better batteries. Batteries are a sort of equipment that store chemical energy and convert it to electrical energy. The study of batteries is receiving increased funding, and battery technology is advancing, but these advancements are all based on research that was conducted on lithium, the third element in the periodic table, four decades ago. Lithium is a very light metal that belongs to the group alkaline, and it has three electrons and the electronic configuration 1S2 2S1, which is due to the presence of just one electron in the outermost shell. Among all the elements, Li has the most ionisation energy. Apart from the fact that each Li-ion cell can generate a very high voltage up to 4 volts as opposed to merely 1.5 volts with conventional cells, this makes material a good candidate for an anode. This is because high reactivity metal. Graphite serves as the cathode and Li Cobalt Oxide serves as the anode in this battery (Fig. 1), with Li pf6 serving as the most popular electrolyte. When a metal oxide electrode is attached, the charging Li atom becomes ionised and splits into a Li ion and an electron, which is the principal function of the electrolyte: to stop the flow of electrons through it towards the negative terminal. Li atom electrons are drawn to the positive battery terminal, travel via the external circuit, and then settle on the graphite. As a result of the loss of electrons, the Li ions become positively charged and are drawn to the battery's negative terminal, where the electrolyte flows. All of the Li ions flow from the anode to the cathode in the fully charged battery as they combine with the Carbon in the graphite to form lubricated carbon, which is then trapped in the cathode. The unstable lithium in the cathode of the battery splits once more into the Li+ ion and electron when it is linked to an external circuit. Now, through the external circuit, electrons are flowing once more from the cathode to the anode, creating electricity. The Battey Li-Cobalt Oxide material is coated with an aluminium current collector to further boost conductivity, and graphite is coated with a copper current collector to facilitate the passage of electrons. Although Li-based batteries have a long lifespan, their capacity degrades over time as a result of the development of solid electrolyte interfaces.

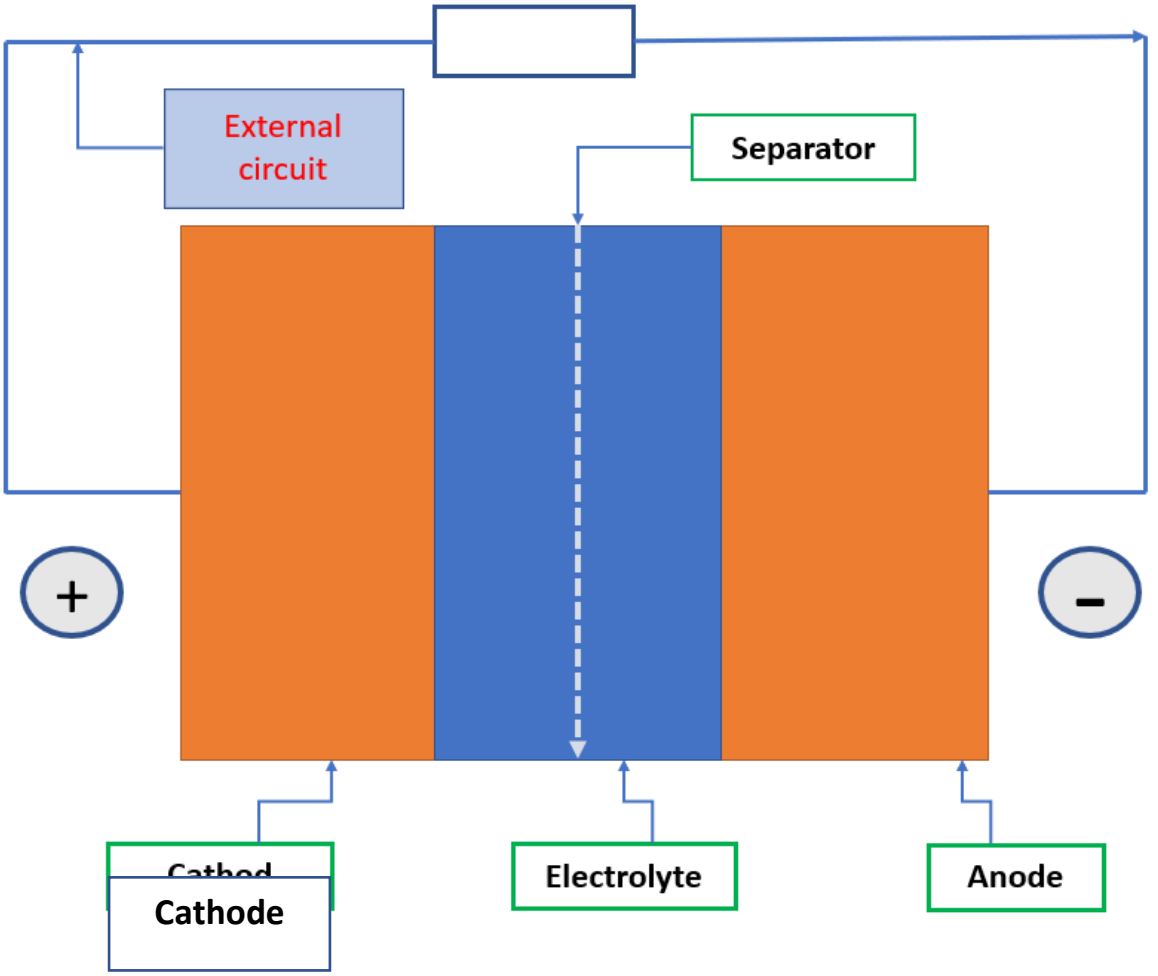

Fig-1: Parts of Li Battery

1.3 Charging and Discharging of LIB:

1.3.1 Charging of LIB:

The electrons are drawn to the positive terminal of the power source once it is connected to the metal oxide terminal (cathode), travel through an external circuit, and eventually reach the layers of graphite. The positive-charged Li-ion will flow through the electrolyte and be drawn to the negative terminal in the interim. Li-ion is trapped in the graphite layer as soon as it reaches there. The cell is completely charged when all of the Li-ion has reached the graphite sheet.

1.3.2 Discharging of LIB:

Li-ion in the graphite layer wants to return to their stable state as the components of the metal oxide as soon as the power supply is disconnected and the load is applied. On the other side, a load is how electrons travel across external circuits. Thus, an electrical current that can be put to use for a variety of things passes through the load. It's important to remember that graphite plays no part in these chemical processes. It only serves as a medium for storing Li-ions.

1.4 Thermal Runaway of LIB:

Battery heating and cooling are greatly influenced by battery thermal management. It can ensure that the battery operates at the right temperature and reduce temperature dispersion within the battery. Thermal runway is a technique that involves accelerating the rise in temperature before releasing energy to raise the temperature even more. Uncontrolled temperature can sometimes result in explosion and self-ignition. Temperature has a significant effect on how well lithium-ion battery cells work. When they are too cold or too hot, they don't function correctly, which can cause severe, long-lasting harm to the cells and quicken their deterioration. Due to the high internal temperature of lithium-ion batteries while operating, there is a high temperature impact. The possibility of a thermal runway exists when the critical temperature (60^0C) is attained. In a battery, it triggers chain reactions which causes self-heating.

Preventing temperature extremes, guaranteeing adequate battery performance, and accomplishing the desired life cycle are the reasons why a thermal management system in the battery is essential. Cell temperatures are maintained within their acceptable operating range using an efficient thermal management system for batteries. In EV batteries, current flow, both during charging and discharging, heats up the cell and the system that connects it. As a part of thermal management, cooling agents can be used in a variety of ways to control temperature. Air cooling, liquid cooling, refrigerant cooling, and other methods are some of them. By using outside air and the movement of the vehicle, an air-cooling system

cools the battery. Adding fans and blowers can improve the cooling effect. The coolant is used to transfer heat from the battery and pump to an air-to-coolant heat exchanger, like a radiator, where it is released into the atmosphere.

1.5 Optimization of BTMS (Battery Thermal Management System):

Finding the conditions that maximise or minimise the function is known as optimization in mathematics. Every design should be improved; this may include the engine, the time, the power consumption, the amount of waste, etc. The words "maximise" or "minimise" are frequently used in optimization problems. The derivative approach makes it simple to identify the right answer when there are boundaries restricting the viable solutions for basic problems or when there are limits or constraints on the resources involved in the optimization. For increasingly complex problems, it may be challenging to quickly recognise the right answer; guessing and checking may take an excessive amount of time; and it may be challenging to locate the values where the derivative equals zero. For the majority of optimization issues, we must employ a special type of program called optimization algorithm. Decision variables and the objective's function are the key elements of optimization. The value that we are attempting to maximise is the objective function. One of the primary objectives of optimization is to improve the value of the objective function through minimization, maximisation, or bringing it closer to a particular value. The gradient and derivatives describe the direction in which the slope of the function grows or declines. The term "constraint" refers to boundaries that the optimizer cannot cross or extra requirements that must be satisfied for a successful solution. Constraints can be divided into two categories: equality constraints and non-equality constraints. Less than equal to form is typically used to express non-equality constraints.

Heat generation and deterioration are the primary issues with lithium battery cells. These issues depend on a wide range of operational factors and are, of course, nonlinear. Minimizing temperature gradient change will enhance the life of the battery cell and the performance of the shell and is a major goal in the design and increased usage of battery

shells. A battery pack with 100s to 1000s of lithium-ion cells adds another level of complexity to the issue. Degradation is high because battery pack temperature gradient is quite great and battery cells cannot properly reject heat due to their dense placement. First, it is important to be able to gauge how well a cell can reject heat. There are two main techniques to do this. The second step is to remodel cells to maximise internal thermal pathways. There are two different kinds of cooling techniques: 1. surface cooling, 2. tab cooling. The average battery temperature is lower with tab cooling than with surface cooling, but tab cooling is more popular nowadays because it maintains a consistent temperature gradient throughout the battery, which is crucial for maintaining battery longevity. We must also seek for the battery's least energy consumption when cooling it. Therefore, the primary goals of battery pack optimization are to reduce pressure loss and improve temperature gradient throughout the cooling channel.

CHAPTER-2

2. LITERATURE REVIEW:

After discussing about thermal runaway of LIB and optimization significance, now we are in a position to talk about different cooling systems which can be employed to cool the battery pack. Now one by one we will see different types of cooling methods.

CLASSIFICATION OF BTMS:

Different types of cooling systems are there which we will discuss briefly along with few research papers through which I gained all useful insides about those.

Here is one diagram (**Fig-2**) shown below about those various cooling systems.

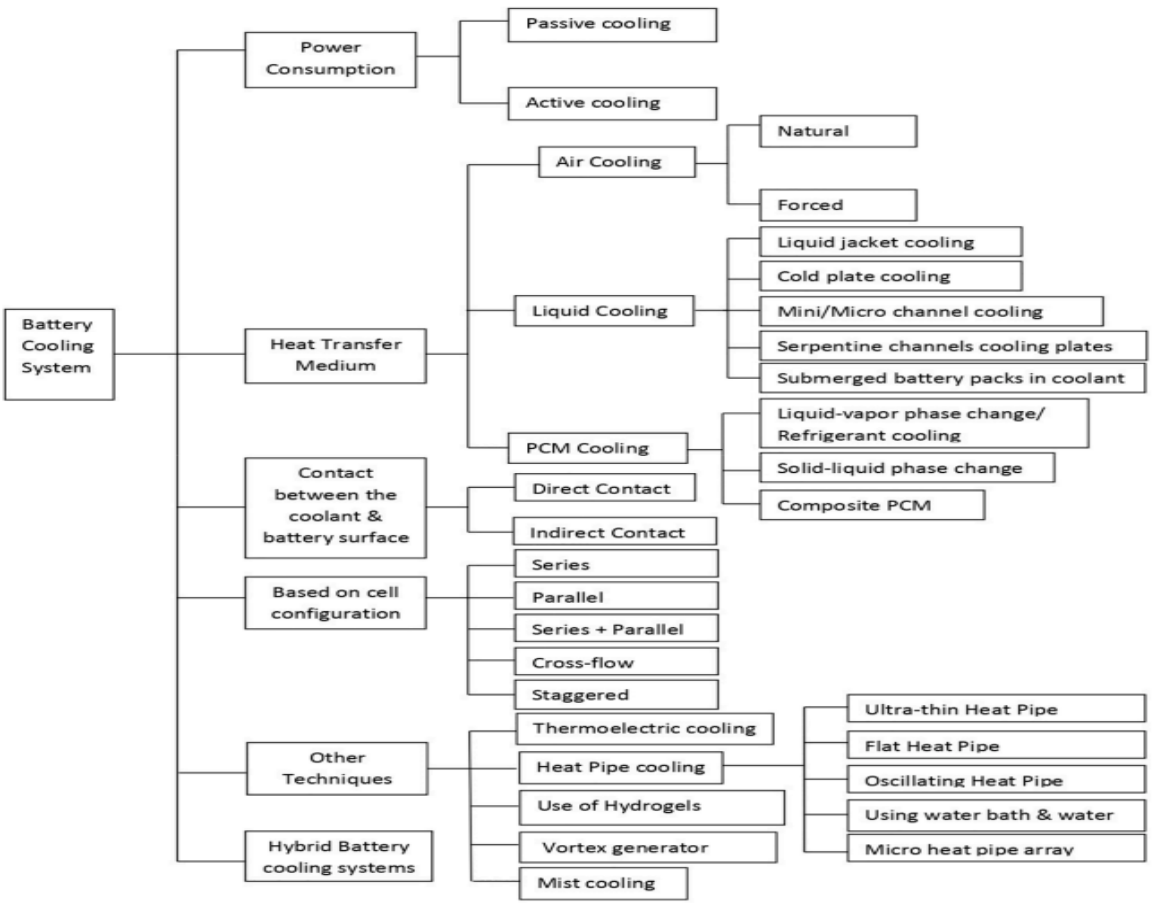

Fig-2: Battery cooling systems classification

2.1 Review on Cooling Methods:

One by one we will discuss about various cooling techniques:

2.1.1 Phase changing materials (PCM) for LIB:

The LIB pack's intercellular spaces are filled with PCM, which is in direct touch with the cells. Additionally, PCM is in direct touch with the conducting plates from the left and right as well as the top and bottom. Heat is released into the environment by these conductive plates. Heat is released as batteries are being charged or discharged. The heat released is initially taken in as sensitive heat, and then a significant quantity is taken in as latent heat at a steady temperature. Therefore, PCM has the ability to cool the batteries under extreme thermal load without causing an anomalous temperature rise or uneven temperature distribution. The temperature then rises as heat is transferred until the entire PCM has changed from a solid to a liquid. Additional cooling is used to deal with the problem, which can release PCM heat into the surrounding area.

J Kim et al. [5] revealed that high thermal conductivity, high heat capacity, high latent heat, and a phase-changing temperature that falls within the operational range should all be present in PCM. It needs to be non-toxic and chemically stable. The addition of thermally conductive material to PCM, metal fins, and porous materials such expanded graphite matrix could all result in the required properties.

2.1.2 Liquid Cooling for LIB:

The battery is cooled using a liquid coolant, such as ethylene glycol, water, or a refrigerant. The liquid passes through tubes, cold plates, or other parts that are placed around the cells and transfer heat to a radiator or another device.

Ke Li [3] used an electro-chemical thermal model to investigate the lithium battery's thermal management system (both computationally and experimentally). He discovered that water cooling provided significantly better results than phase change material (P.C.M) cooling at lower cycling rates.

Bai et al. [8] used Phase change material and water-cooling plate to improve the performance of lithium-ion batteries. The cooling plate was used to improve cooling performance, while the phase change material was used to maintain consistent battery temperature. Additionally, they found that increasing inlet flow outperforms all other methods of cooling batteries, and that cooling plate height may be adjusted to minimize energy usage in the region between batteries.

2.1.3 **Heat Pipe Cooling for LIB**:

Heat pipe is a device that can move heat on its own, without the need for any additional power sources. It is made up of an evaporator, an adiabatic, a condenser, and a wick. The heat point (heat source) where the liquid working fluid of the heat pipe absorbs sand evaporates is connected to the evaporator portion. Due to the internal pressure differential, the evaporated working fluid then travels via the adiabatic portion to the condenser section. The working fluid exchanges heat with the condenser's heat exchanger before condensing. The working fluid is once more carried to the evaporator by the capillary action of the wick after becoming a liquid. This is how a heat pipe functions.

Li et al. [15] investigated the TR of a LIB numerically using heat pipe cooling. The VOF method of ANSYS FLUENT was used to model the heat pipe. UDF was defined and assembled in ANSYS FLUENT for the heat-mass transfer in the heat pipe between the evaporator and condenser section.

The numerical analysis revealed that the heat pipe cooling approach was unable to stop TR in a single LIB. Although heat pipe cooling can stop TR from spreading from one LIB to another.

Chen et al. [9] and his colleagues constructed an electro-chemical thermal model and ran simulations in ANSYS using various cooling techniques. They discovered that indirect liquid cooling produced the best results, while direct liquid cooling was more feasible. Fin cooling will make the system heavier overall, while air cooling will take the most power (because of high mass flow rate).

Z Lu. [10] investigated a variety of methods to enhance the cooling performance of a dense lithium-ion battery pack cooled by forced air and discovered that increasing the coolant channel size could produce better results but would undoubtedly complicate the design, which is a disadvantage.

Duan et al. [15]. Put forth various cooling solutions to regulate battery cooling. Although decreasing inlet flow temperature is demonstrating good results for thermal management, it should be optimised because it would increase power consumption. Thermal contact resistance between the battery and cooling channel should also be taken into account.

2.1.4 Air Cooling System for LIB:

BTMS utilises an air-cooling system due to its simple construction and inexpensive maintenance. Air from the evaporator, preconditioned air from the cabin, or ambient air from the outside can all be used as a cooling source. The air source is chosen based on heat generation, surrounding conditions, and driving propensity. Air cooling systems are less efficient because of their limited thermal conductivity and heat capacity. Other drawbacks of this technology include its limited capacity for batteries due to the need to maintain an appropriate air space between batteries. The system is huge and noisy because it uses an integrated system of ducts and fans to circulate a large volume of air for effective cooling. To enhance the cooling system's performance, research is being done. To increase the system's efficiency, changes are made to the cell configuration, airflow pathways, and air channel design.

Rajib Mahamud and chanwoo park introduced two types of air cooling in his paper , one was unidirectional and another was reciprocating air flow for LIB cooling considering 2D simulation of LIB pack of 8 batteries(capacity of 3.6 Ah each). The experimental findings from in-line tube-bank systems, which closely resemble the battery cell configuration taken into account for this study, were used to validate the CFD model's findings. In comparison to the uni-directional flow example ($=\infty$), the numerical results demonstrated that the reciprocating flow may lower the battery system's cell temperature differential by approximately 4^0 C (72% reduction) and the highest cell temperature by 1.5^0 C for a reciprocation duration of 120 seconds. This temperature increase is attributed to the periodic flow reversals' periodic heat redistribution and disturbance of the boundary layers that form on the cells.

Zukauskas and R.Ulinskas at the Academy of Sciences of the Lithuanian SSR's Institute of Physical and Technical Problems of Energetics, a significant programme of heat exchanger research has been going on for a while. Currently, a variety of 150 banks have been

researched over a wide range of flow velocities, fluid physical characteristics, Reynolds numbers (from 1 to 2 X 10^6), and Prandtl numbers (from 0.7 to 10^4). The results of the experiment have been interpreted in a variety of ways, and methods for assessing how fluid physical qualities affect heat transport have been studied. From his paper we validated Re vs friction factor graph with our CFD Results.

Wang et al. [8] experimented air cooling of an 18650 Li-ion cell (Panasonic NCR18650PF; C/LiNiy-MnzCo1-y-zO2, NCM) at various charging and discharging rates. Additionally, he contrasted two LIB module cases: one with an above opening for cross ventilation and the other with a bottom opening for cross ventilation. He evaluated the LIB's safety based on two factors: the temperature difference (TD) within the LIB module and the LIB's maximum temperature. According to the analysis, case 1's upper cross ventilation is more effective than case 2's bottom cross ventilation at maintaining the TD and maximum temperature within a safe range (case 2). In addition, it was discovered that LIB becomes more susceptible to TR when the discharge rate increases, from 1C to 2C.

Bubbico et al. [7] performed an experimental analysis on the effect of the velocity of air on the cooling of single LIB and the LIB pack. The air velocity in the four cells that make up the LIB module ranged from 0 to 7 m/s. Beyond 4 m/s of air velocity, it was discovered that the LIB pack was safer. Additionally, it was discovered that raising the velocity reduced the temperature gradient inside the LIB module and allowed LIB to be maintained at a safer temperature limit.

Chen et al. [9] performed three dimensional CFD analysis on the performance of air as cooling on thermal and pressure drop perspectives. He carried out the analysis for two designs: the pin-fin channel design, where air is in direct contact with the LIB cell surface, and the fin outside design, where a metal plate with a fin structure is positioned between

the LIB surfaces without any air movement. Two heat generation cases, 500W for normal load and 1500W for peak load, were examined. It was discovered that a higher air flow rate might keep the LIB within the safe temperature range (308 K). Fin outer design performs better than the other cases. The LIB module becomes increasingly hazardous as the air inlet temperature rises. Higher thermal conductivity metal panels were found to preserve temperature homogeneity. However, this effect started to fade at 2000 W/(m 0K).

2.2 Objectives and Literature Gap:

After all these discussions about different cooling techniques & thermal runaway concepts and many more related topics, we are now in a position to talk about what could be the best possible solution for LIB thermal management. We have chosen Air cooling as our cooling medium because of its simple design and very less maintenance.

- To develop a 2D model of stack of 8 cells and validate with the literature of unidirectional flow cooling.
- To simulate the cooling of battery by introducing sinusoidal velocity profile as inlet.
- To perform a comparative assessment for cooling of batteries with unidirectional constant velocity profile and unidirectional sinusoidal velocity profile.

Chapter-3

3. Numerical Modelling

3.1 Governing equations

For solving conjugate heat transfer problem there are two zones working

1. **Battery zone**

In battery domain generalized heat conduction equation is used (assuming battery is homogeneous and isotropic).

$$\frac{\partial}{\partial x}\left(k\,\frac{\partial T}{\partial x}\right)+\frac{\partial}{\partial y}\left(k\,\frac{\partial T}{\partial y}\right)+\frac{\partial}{\partial z}\left(k\,\frac{\partial T}{\partial z}\right)+\dot{e}_{gen}=\rho\,c\,\frac{\partial T}{\partial t}$$

k=thermal conductivity of battery

$\dot{e}_{gen}$= heat generation/volume c=specific heat of battery

ρ = density of battery zone

2. **Air zone**

In this domain Navier Stokes equation is used, there are three equations for Navier stokes.

a) **Continuity equation**

∇ = gradient operator

u = velocity component of air

ρ=density of air (assuming incompressible flow)

$$\frac{\partial \rho}{\partial t}+\nabla.(\rho u)=0$$

Or, $\nabla.u=0$

b) Momentum equation

$$\frac{\partial u}{\partial t} + (u.\nabla).u = -\frac{1}{\rho}\nabla p + F + \mu\nabla^2 u$$

u=velocity component of air

ρ=density of air

F=body force

μ=viscosity of air

c) Energy equation

$$\frac{\partial(\rho \mathrm{Cp} T)}{\partial t} + (u.\nabla)(\rho \mathrm{Cp} T) = \nabla.\left(K_f \nabla T\right)$$

E=Total energy of air (thermal energy + mechanical energy)

K_f = thermal conductivity of air

3.2 Battery Modelling:

This analysis was done by taking a cylindrical Li-ion cell of 3.6Ah capacity and having Diameter*Length(D*L=42.4mm*97.7mm). To get best possible result we selected 2 Dimensional CFD model for our LIB. Instead of using the battery submodule centerline, the symmetric planes between the battery submodules were selected. This is due to the asymmetric flow that results from the creation of Karman vortexes at high Reynolds number conditions behind the final cells. In order to prevent evolving velocity circumstances from impacting the computation results, the computation domain additionally contains an additional flow zone that is extended from the battery area. Including the portion of the battery cells (l_b = 413.4 mm), the computational domain of the battery system has a total

length (l_t) of 1060 mm in the streamwise direction. The battery area's left side extension measures 323.3 mm in length, while the right-side extension measures 323.3 mm in length. The battery submodule has a 53 mm width (w). The Diameter of the battery is 42.4 mm. **Table 1** is a list of the dimensions and specifications of the battery system taken into consideration for this investigation. Due to the cylindrical battery cell's layered-film design, only radial conduction in the battery cells was taken into account for this investigation.

Table-1: **LIB cell specifications:**

Sl.no.	Parameters	Units	Values
1	Capacity	Ah	3.6
2	Diameter (D)	mm	42.4
3	Length (L)	mm	97.7
4	Mass (M_c)	Kg	0.3
5	Area (A_{ku})	mm^2	13014
6	Volume(V_c)	mm^3	137948.2
7	Density(ρ_c)	kg/m^3	2007.7
8	Thermal Conductivity	W/m-K	32.2
9	Specific Heat(C_{pc})	J/kg K	837.4
10	Entropy Coefficient(dE/dT)	mV/k	-0.3
11	Number of cells in flow directions(n)		8
12	L_i	mm	323.3

13	L_o	mm	323.3
14	L_b	mm	413.4
15	L_t	mm	1060
16	Charge/ discharge rate	C	7
17	S_t	mm	53
18	S_l	mm	53
19	Width(w)	mm	53

*Subscript “c” is for Cells.

3.2.1 Creating Geometry and Meshing:

Fig-3 shows the **geometry** files for the battery configuration. Here we took a LIB pack of 8 batteries having diameter 42.4 each and symmetric planes were selected between the battery submodules. The whole geometry was created with the help of ANSYS design modeler.

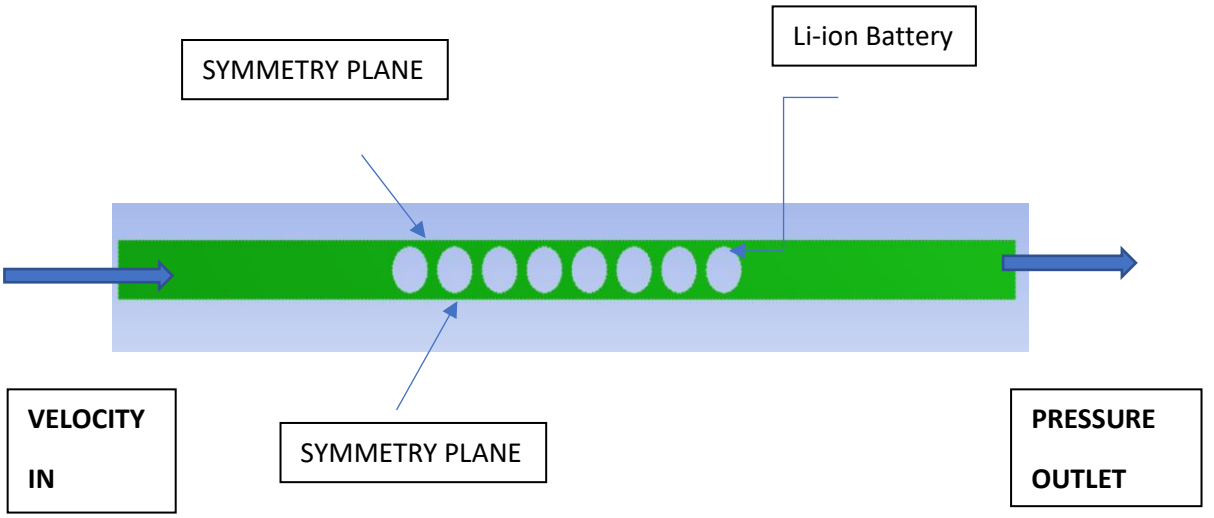

Fig-4 shows the **meshing** part of our model. ANSYS meshing tool was used to discretize the above geometry. Total 197395 nodes and 206792 elements were used to perform this simulation. Element size around the cell walls was kept as 0.05mm as finer mesh was required there and 1mm element size was kept for others like uniform sections where course mesh was the criteria for our study. No meshing was done inside the cells as there were no air flow involved so it could reduce computational cost as well. Face sizing was done for entire faces whereas Edge sizing was applied at the walls of battery cells.

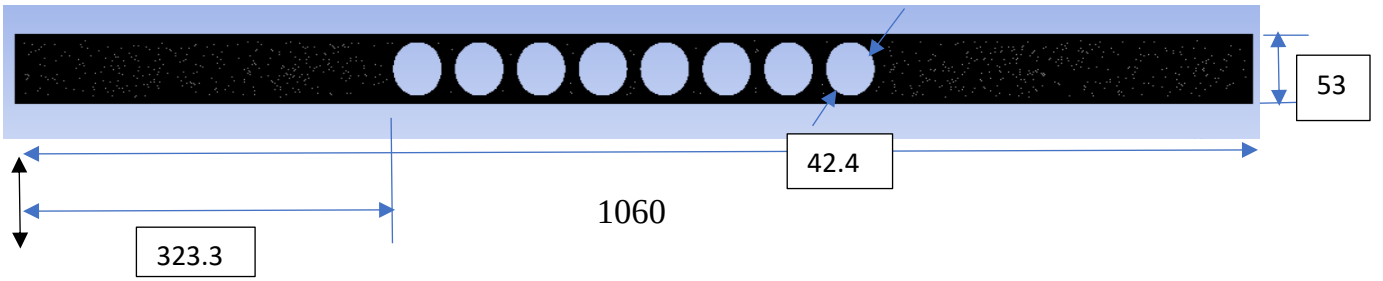

Fig-4: Meshing of LIB pack

*All units are in 'mm'

3.3 Air cooling of LIB pack under Heat generation:

Prior cooling process, we need to understand about heat generation which is taking place inside this LIB pack. This generation can be divided into two parts:

1. Reversible heat generation
2. Irreversible heat generation

We will discuss about those heat generations calculations briefly under next sub-heading. Basically the total heat generation is the sum of these two terms i.e. reversible and irreversible heating.

3.3.1 **Heat generation calculations**:

$\dot{e}_{gen}$= Total heat generation of a battery cell

Where,

$$\dot{e}_{gen} = Q_r + Q_{irr}$$

Q_r=Reversible HG of LIB

Q_{irr}=Irreversible HG of LIB

$Q_r = -IT(dE/dT)$

I= current(amp)

dE/dT=Entropy coefficient =-0.3(mV/K) which was taken from an experimental paper by Zukauskas & Ulinskas.

$Q_{irr} = I^2R$

Where,

$R = -0.0001\ T^3 + 0.0134\ T^2 - 0.5345\ T + 12.407$

T= Temperature of cell in ^{0}C

R= Electrical Resistance in mΩ

3.4 **Computational setup and boundary conditions**:

For this LIB simulation, we considered **transient** flow using **PISO** algorithm. The commercial software **ANSYS FLUENT**, which is based on the finite volume approach, was used to create the two-dimensional CFD model. The buoyancy effect was disregarded for the CFD analysis, the Reynolds stress and renormalization group **(k-€)** was used for the turbulent model, the Navier-Stokes momentum equation was solved using the **second-**

order upstream difference scheme, and the **PRESTO** (pressure staggering option) algorithm was taken into account for the swirling flow.

Few important computational parameters were set to get the most accurate result. We fixed divergence criteria as $\mathbf{10^{-6}}$ for energy equation, $\mathbf{10^{-4}}$ for continuity and momentum equations and 10^{-3} for (k-€) model. Number of iterations per step and total number of steps were then decided as per our air flow time (in sec). We took **0.01 time step size** for our entire simulation and observed this flow for **6000 sec unidirectionally.**

We set fix air velocity of **1 m/s or Re=13300** as inlet boundary condition and kept pressure outlet for our study. Inlet and outlet temperatures of air were set as $\mathbf{20^0C}$ and 27^0C respectively. We created conjugate surfaces in ANSYS setup for each cell where conduction and convection both were taking place. We finally generated surfaces for each interior cell to track temperature variations with flow time and to get the temperature contours. We also created inlet and outlet surfaces to calculate pressure drop with flow time. That pressure drop value was further used in calculation of friction factor. Formula used for evaluating the friction factor was taken from an experimental paper by **Zukauskas and Ulinskas**, written below.

Friction factor, $f=\Delta P/(0.5*n*\rho*U^2_{max})$

Where, ρ= Density of Air

U_{max}= maximum velocity in the least free space=$(S_t/S_t-D)*U$

n=Number of cells

U= Free space velocity

3.4.1 Setup for Air Cooling:

Table-2 represents properties of Air at 300K as shown below.

Table-2: Properties of Air

Sl.no.	Parameters	Value
1	Density(kg/m^3)	1.1614
2	Thermal conductivity(W/mK)	0.0263
3	Specific heat(J/kg-K)	1007
4	Viscosity(kg/m-s)	$1.846*10^{-5}$
5	Prandle number	0.707

For the heat generation inside the battery, a User Defined Function **(UDF**) was used. That UDF was formed by considering all HG terms and applied for each cell as the only heat source for our study. Those HG terms were already discussed under HG calculation portion.

Chapter-4

4.Results and Discussion

4.1 Validation of LIB pack CFD model using Unidirectional flow:

We validated our CFD result of 2D numerical LIB pack model with the experimental results of in line tube bank system by **Zukauskas and Ulinskas** using unidirectional flow**.** Formula for friction factor calculation was taken from that paper only. We got our pressure drop value for inlet and outlet after the numerical computation of our 2D model. That 2D model was taken from one of the air cooling numerical paper by **Rajib M. and Chanwoo P**. We also validated our 2D model results like temperature variation curves for each cell with his numerical results.

4.1.1 Validation of 2D model for friction factor (FF) vs Re plot:

All the formulas and concepts regarding this were already discussed in above topics. We will observe how FF varies with Re using unidirectional flow in **Fig-5**.

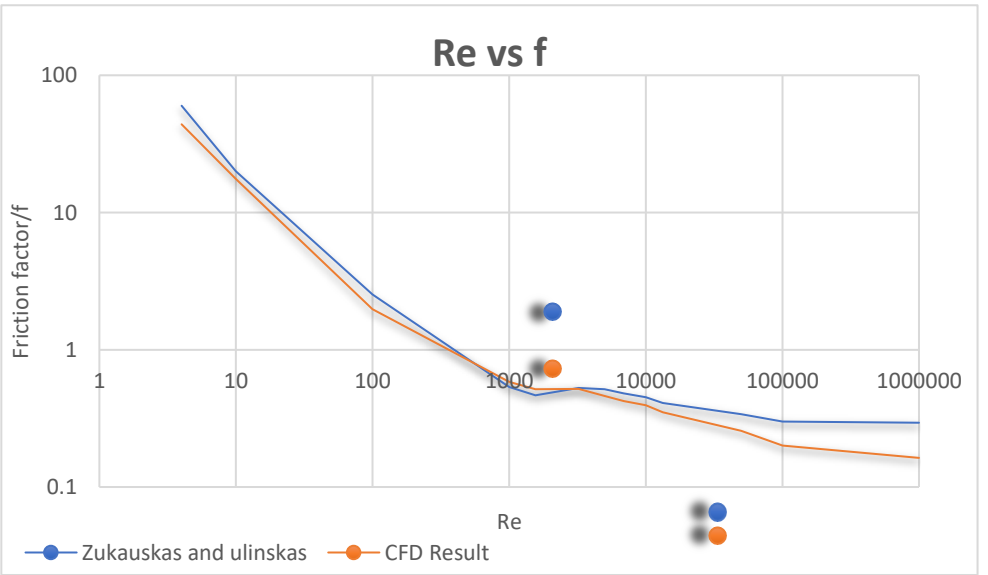

Fig-5: Variation of FF with Re

Calculations of Pressure drop for evaluating FF were done using ANSYS simulation. **Table-3** shows values of FF with different Re below.

Table-3: Values comparison of FF in case of CFD and Experimental results

Re	f exp	f (CFD)
4	**60**	**43.937**
10	**20**	**17.586**
100	**2.53**	**1.98**
1000	**0.535**	**0.583**
1557.59	**0.4652**	**0.516**
3231.72	**0.5265**	**0.52**
5000	**0.517**	**0.461**
6882.34	**0.4819**	**0.424**
10000	**0.45**	**0.394**
13300	**0.41**	**0.35**
50000	**0.34**	**0.256**
100000	**0.2991**	**0.201**
1000000	**0.294**	**0.163**

4.1.2 Validation of LIB pack using Baseline condition:

After this above validation, we took one constant inlet velocity as baseline condition for our numerical analysis. We considered Re of 13300 which was equivalent to 1m/s inlet velocity. Here, we compared our CFD result for temperature calculations in each cell with that air cooling numerical paper

using unidirectional case by **Rajib M. and Chanwoo P.**

We can observe **Fig-6** to understand that how accurate our model was built. **Table-4** shows the values of temperatures for each cell. We used MS EXCEL for making all those required graphs and tables.

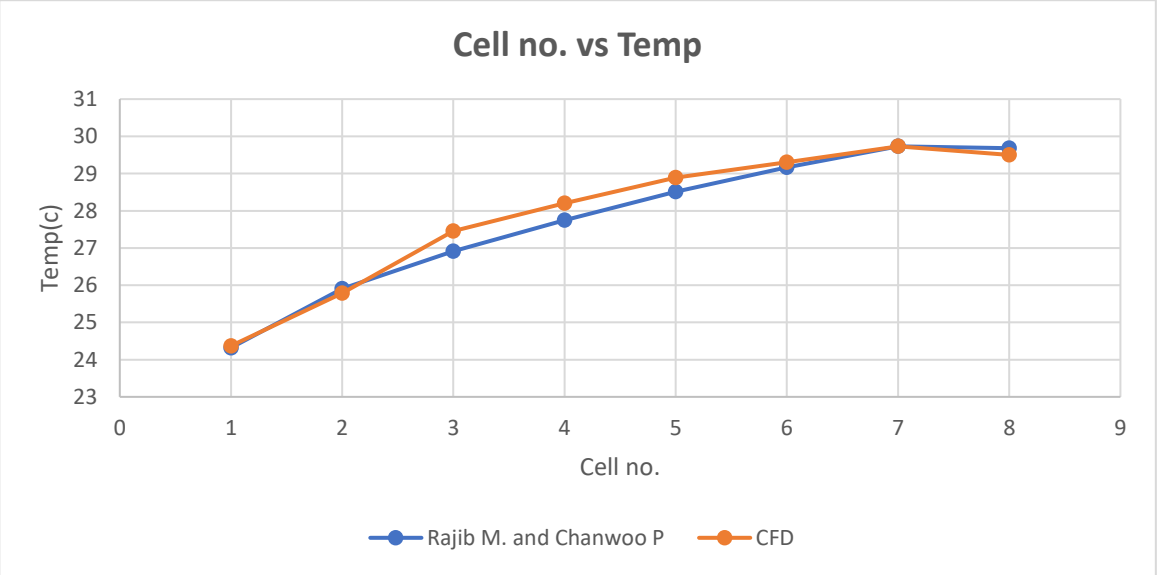

Fig-6: Temperature values for each cell

Table-4: Comparison of cell temperature values

CELL NO.	Temp/^{0}c(PAPER)	Temp/^{0}c(CFD)
1	24.3194	24.37
2	25.9061	25.79
3	26.9081	27.45
4	27.7432	28.2
5	28.5115	28.89
6	29.1628	29.3
7	29.7307	29.73
8	29.6806	29.5

Here we can observe that values of temperature increase from inlet to outlet. Therefore, cell 1 is having lowest temperature. But on this note we could assume that temperature will be highest in cell 8 but it was not the case. Cell 7 is having slightly higher temperature than cell 8. This is because of the exposure to convective zone facing by cell 8 than inner cells hence experiencing bigger recirculation behind the cells.

4.1.3 Temperature contours for LIB pack CFD model:

Fig-7 shows temperature contours of LIB pack of 8 cells CFD model with unidirectional air cooling. We simulated this flow for 6000 sec to track the temperature propagations from inlet to outlet of LIB model.

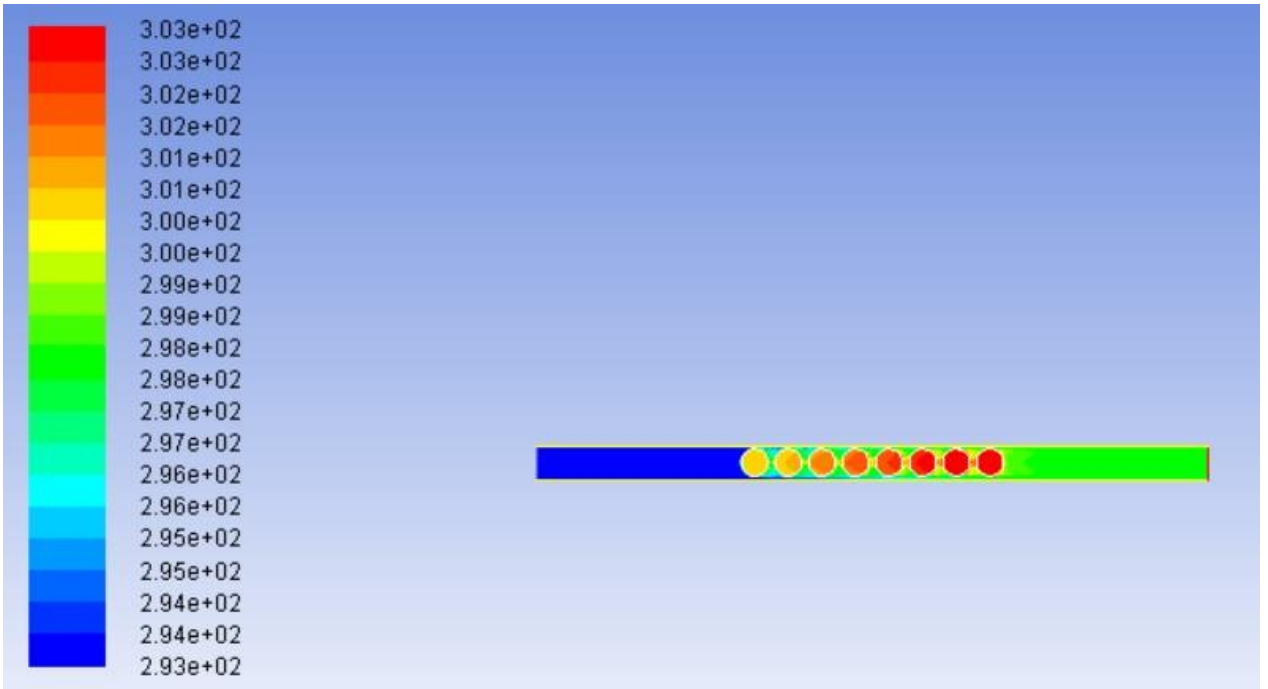

Fig-7: Temperature contours of CFD model for 6000sec unidirectional flow

4.1.4 Validation of cell temperature variations with flow time:

Now we will see the temporal variations of temperatures for each cell one by one. We simulated this result by taking a constant stepwise charge and discharge value of (±25.2A) as current and kept our cycle time for battery as 150 sec in each case.

We considered unidirectional flow case from this numerical analysis paper by **Rajib M. and Chanwoo P.** and tried to validate our result with this.

Fig-8, Fig-9, Fig-10, Fig-11, Fig-12, Fig-13, Fig-14, Fig-15 showing "temporal variation of temperatures" for cell-1, cell-2, cell-3, cell-4, cell-5, cell-6, cell-7, cell-8 respectively.

Cell-1:

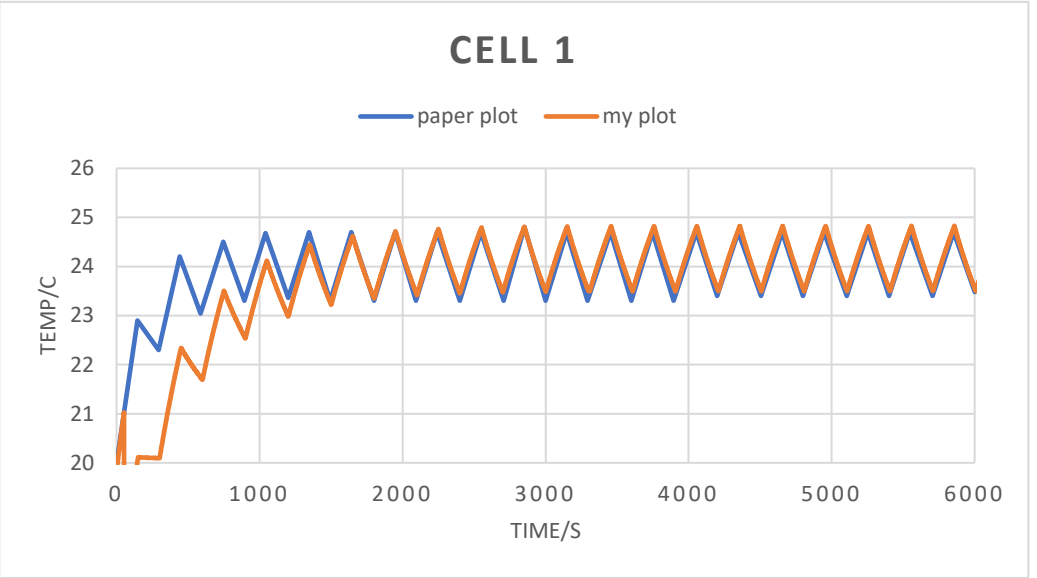

Fig-8: Temperature variation of cell-1 with flow time

Cell-2:

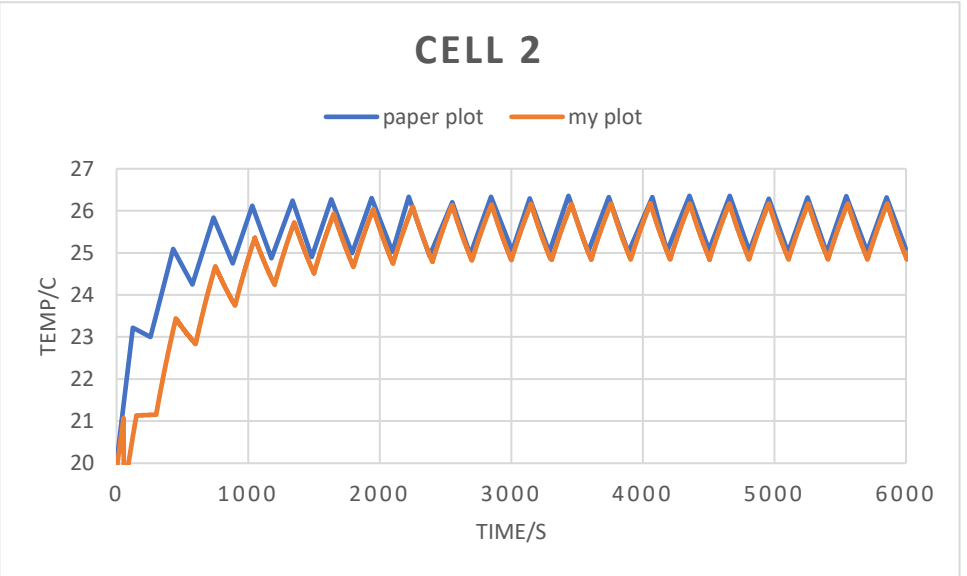

Fig-9: Temperature variation of cell-2 with flow time

Cell-3:

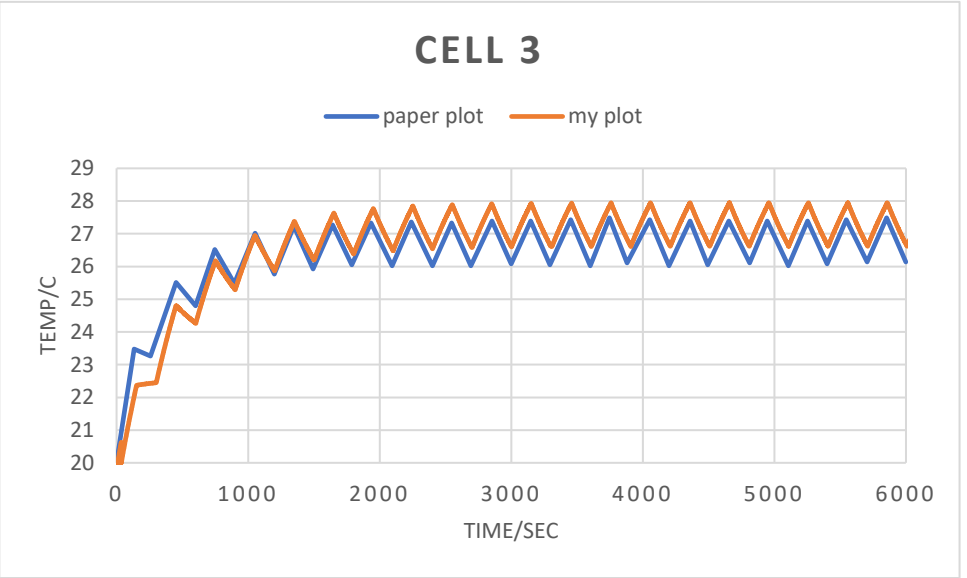

Fig-10: Temperature variation of cell-3 with flow time

Cell-4:

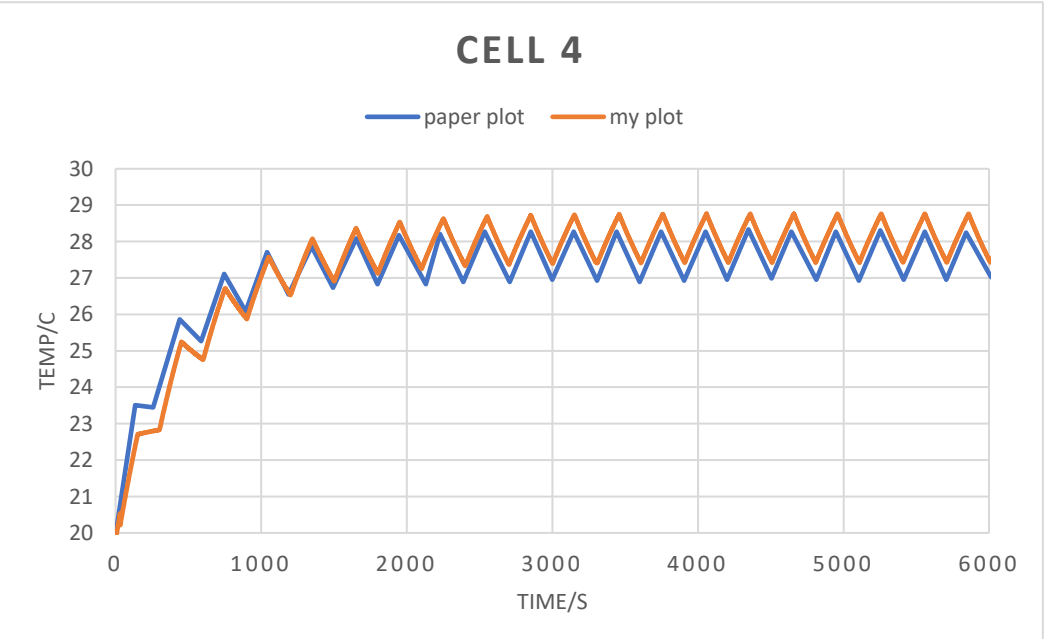

Fig-11: Temperature variation of cell-4 with flow time

Cell-5:

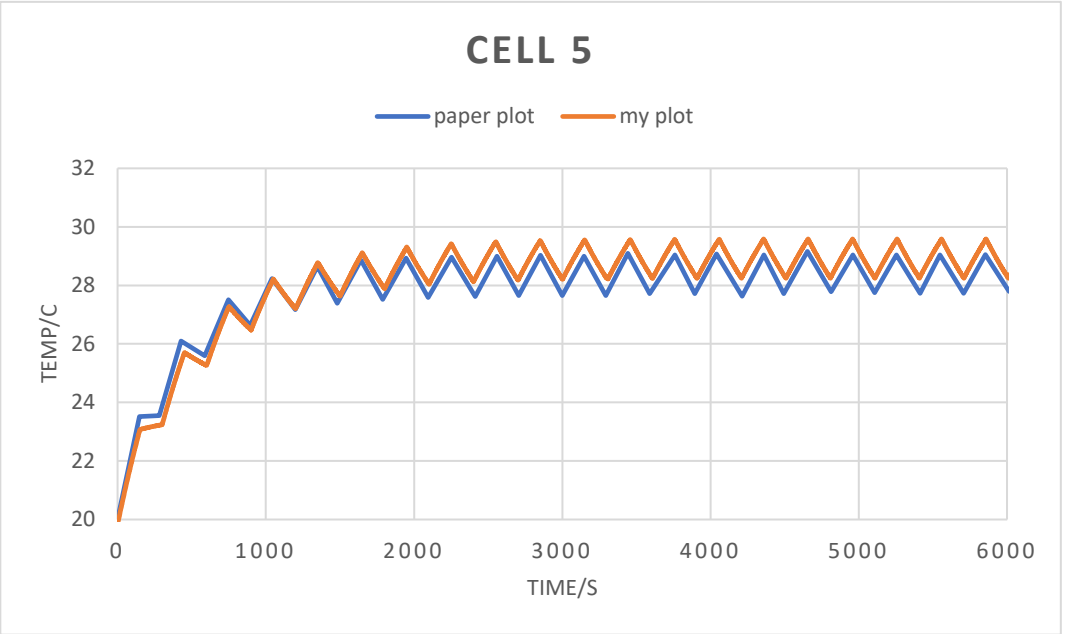

Fig-12: Temperature variation of cell-5 with flow time

Cell-6:

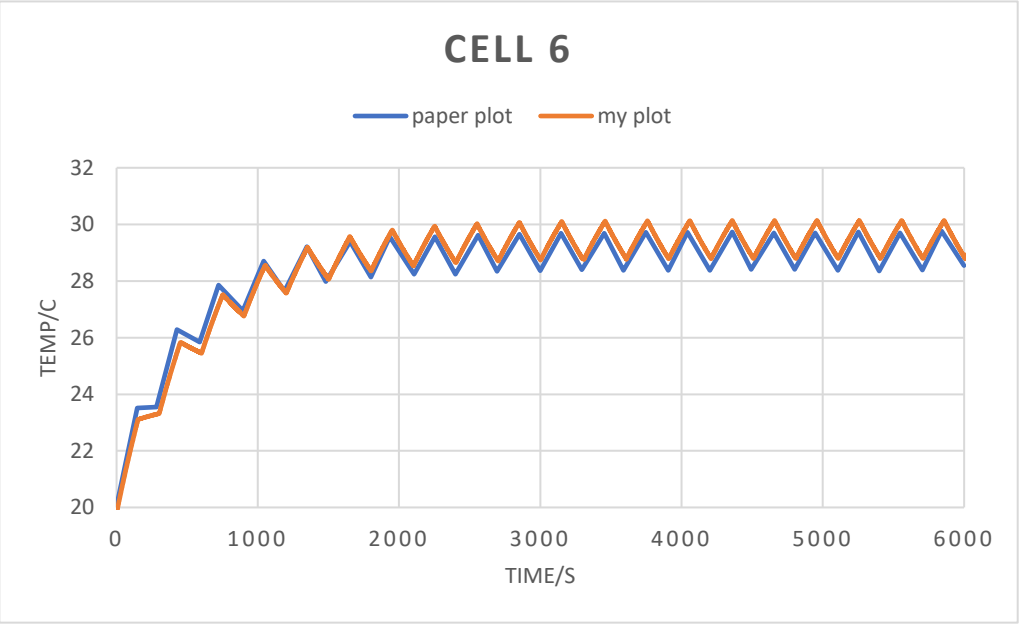

Fig-13: Temperature variation of cell-6 with flow time

Cell-7:

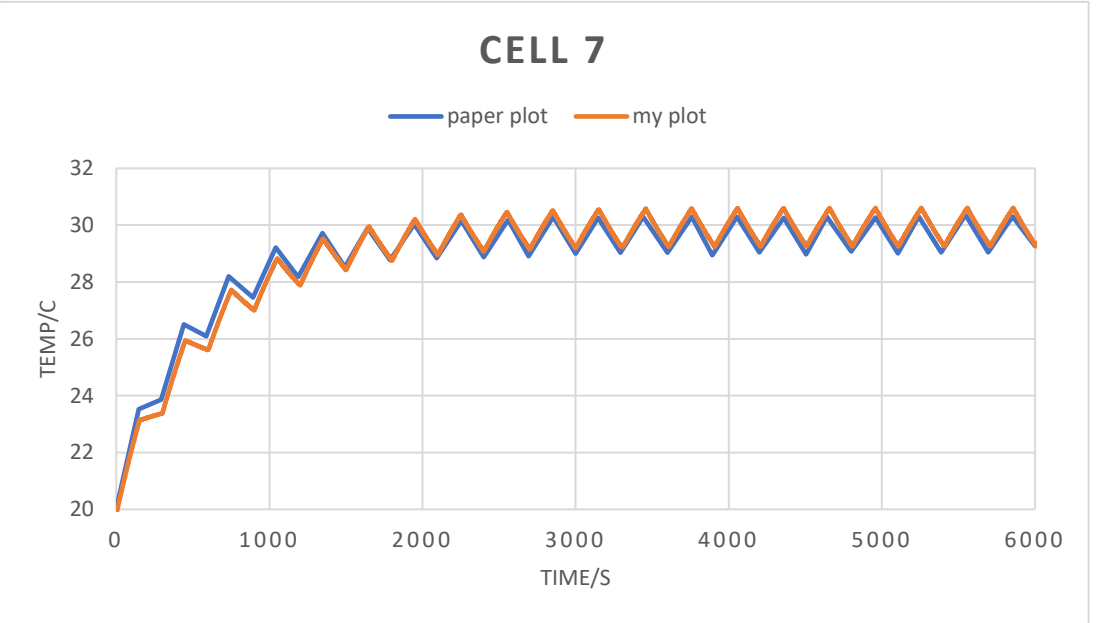

Fig-14: Temperature variation of cell-7 with flow time

Cell-8:

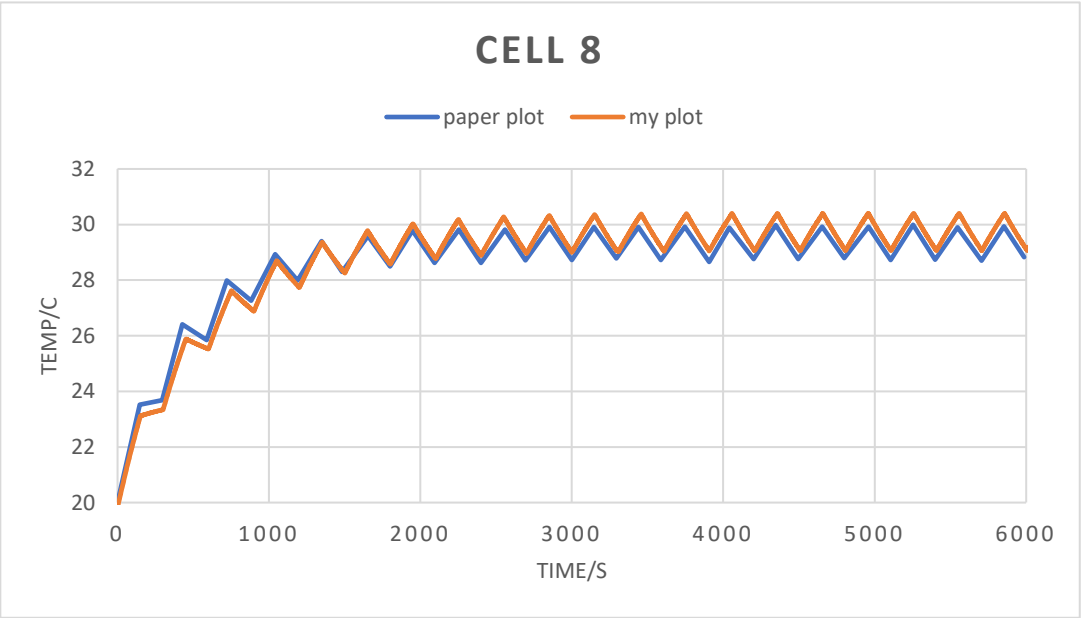

Fig-15: Temperature variation of cell-8 with flow time

4.2 Results:

4.2.1 Applying Sinusoidal inlet velocity profile:

We have already covered validation portion in detail. And we have also come across all the graphs and results which we got after validating our LIB pack CFD model.

Now we have done some modifications in our boundary condition. We took inlet velocity as Sinusoidal profile instead of constant rectangular velocity profile. We kept our geometry and meshing same as before which we already explained in previous topics.

We will now analyze our result for current boundary condition. We simulated our flow for 4000 sec and took time step size as **0.005** for accurate result. Rest of the conditions were same as before. Our aim is to increase heat transfer and to achieve better thermal management of this LIB pack. Let us now discuss whether our goal is fulfilled or not.

4.2.2 Temperature variations for each cell:

Fig-16 shows how temperature varies with flow time (in sec) for each cell after applying sinusoidal inlet boundary condition. This plot clearly indicates that maximum temperature with sinusoidal inlet boundary condition is much higher than the rectangular BC.

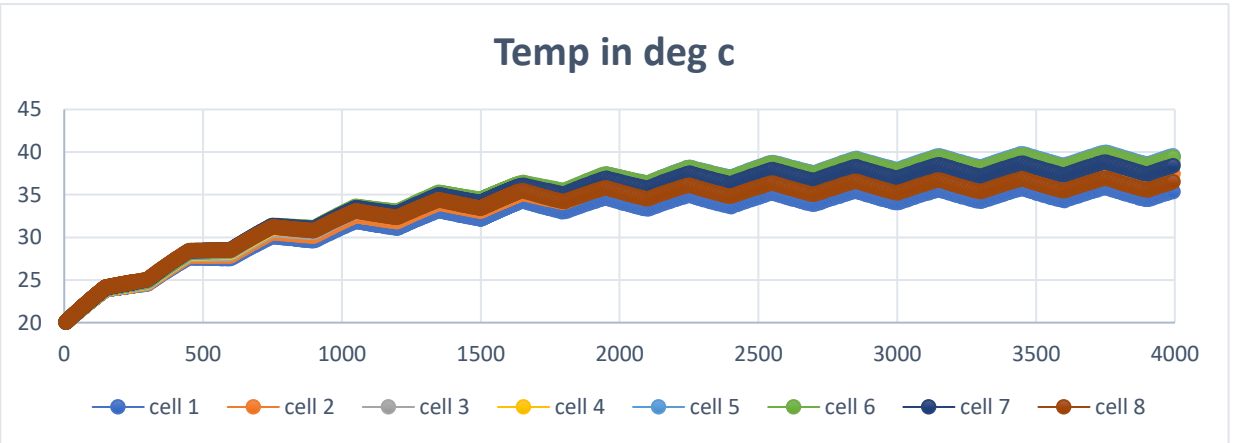

Fig-16: Temperature variations for all cells with sinusoidal inlet condition

Here we can see that temperatures are very close to each other for cells unlike constant rectangular velocity profile.

4.2.3 Temperature contour with sinusoidal inlet BC:

Fig-17 represents temperature contour of whole region with inlet sinusoidal velocity condition. After analyzing this temperature contour, we got some very important observations. We came to know about maximum temperature and maximum temperature difference for cells in **Fig-18** where cell number vs temperature is shown. At inlet air temperature was 20^0C. As we proceed from cell 1 to cell 8, we can see temperature got increased as expected but in case of cell 8 temperature was lesser than cell 7 and even cell 6. It is because of convective zone around cell 8. We can also see that temperatures of cells are very close to each other. Propagation of heat from inner cell to outer cell is not desirable as inner cells are having higher temperature.

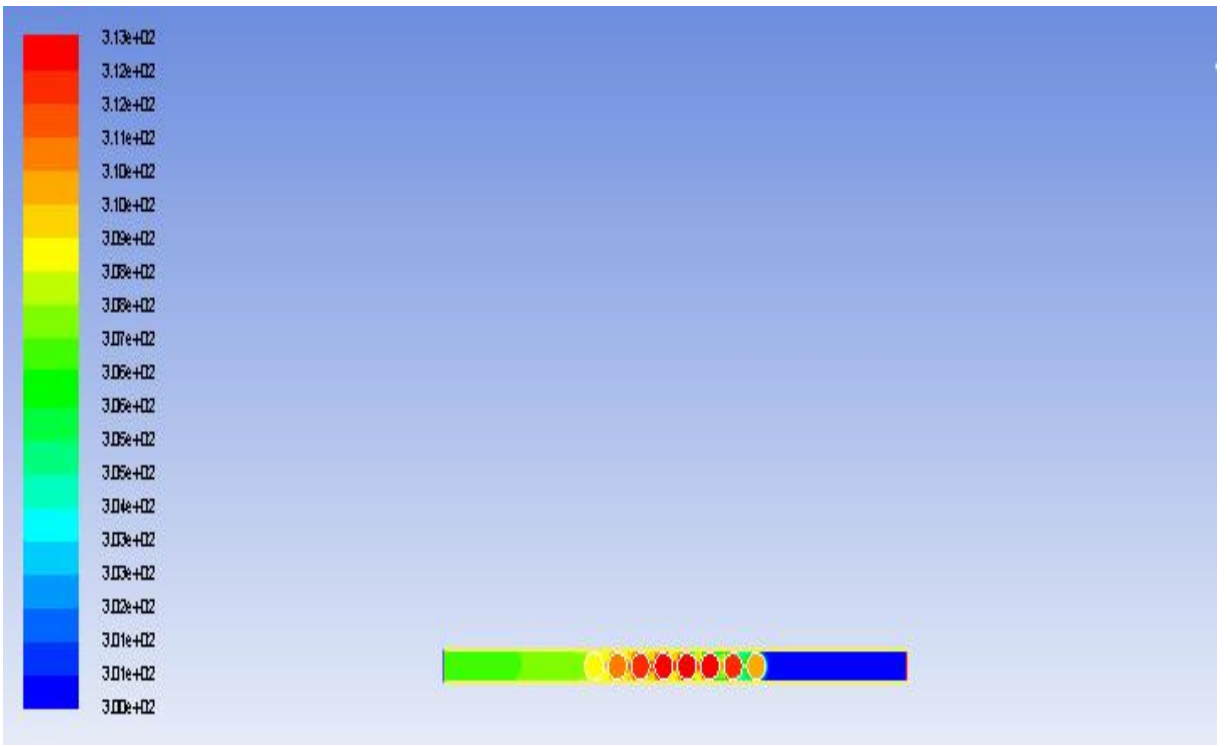

Fig-17: Temperature Contours with sinusoidal inlet condition

4.3 Comparison of results between rectangular and sinusoidal inlet condition:

In case of LIB pack cooling using unidirectional flow with rectangular inlet velocity condition, we got maximum temperature as 29.73^0C and maximum temperature difference (MTD) as 5.36^0C. Whereas we got 39.7^0C as maximum temperature and MTD as 4.28^0C. **Fig- 18** shows the comparison of results between two inlet boundary conditions.

After all these simulations for LIB pack CFD model, we can easily observe that temperature is much higher in sinusoidal case. **Table-5** represents the values of temperatures with cell number in case of both conditions.

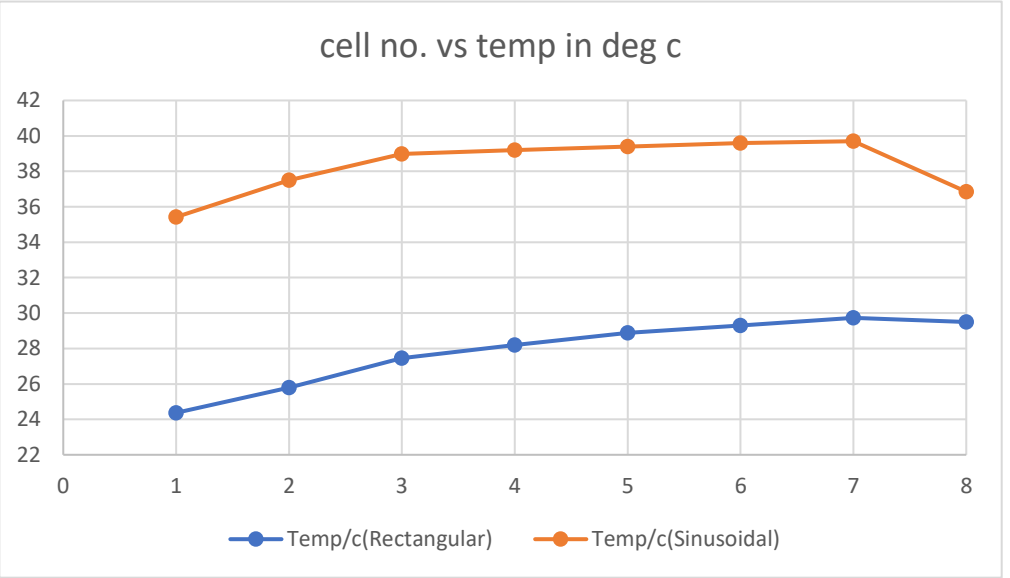

Fig-18: Comparison of cell number vs temp for two inlet velocity profiles

Table-5: Values comparison between two inlet velocity profiles

CELL NO.	Temp/c(Rectangular)	Temp/c(Sinusoidal)
1	24.37	35.42
2	25.79	37.5
3	27.45	38.98

4	28.2	39.2
5	28.89	39.4
6	29.3	39.6
7	29.73	39.7
8	29.5	36.85

4.3.1 Comparison of temperature variations with flow time in both velocity conditions:

Cell-1:

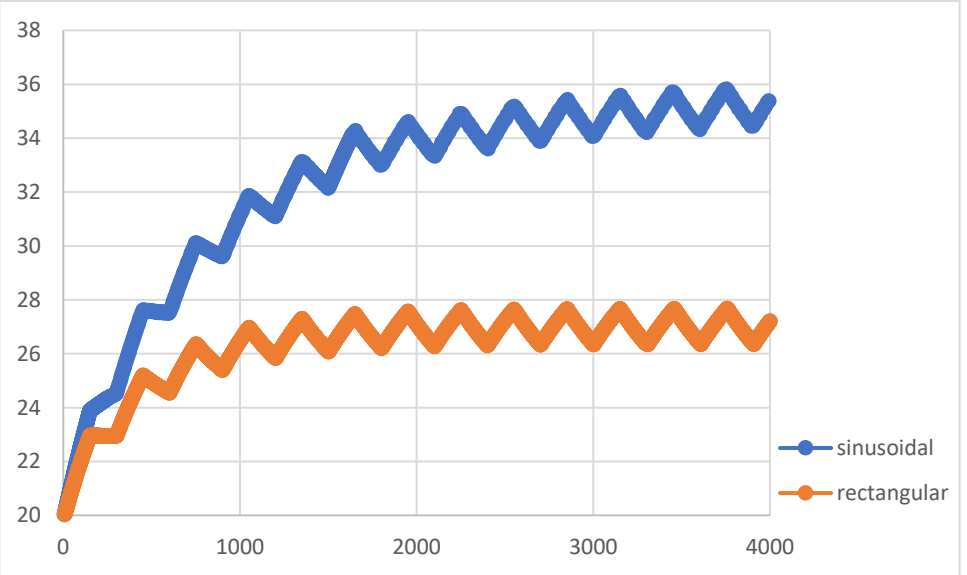

Fig-19: Comparison of two inlet BC for cell-1 Temperature variation vs flow time

Cell-2:

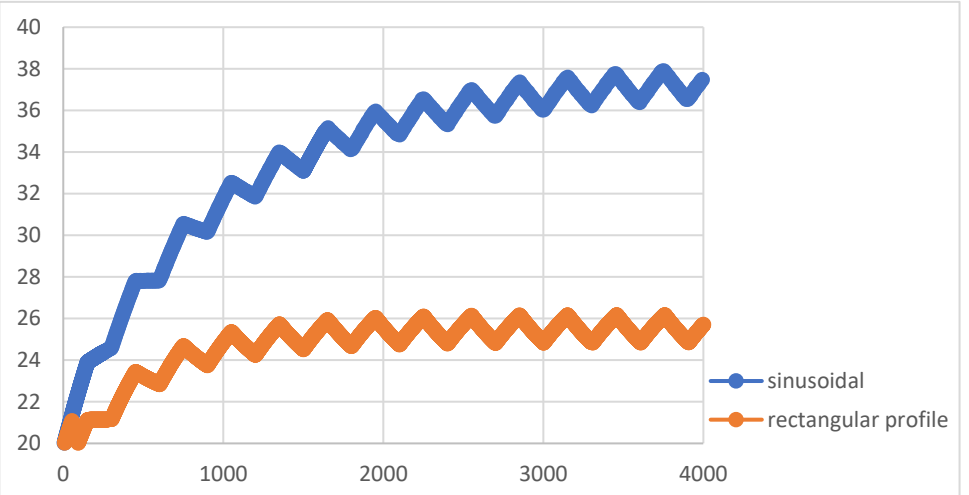

Fig-20: Comparison of two inlet BC for cell-2 Temperature variation vs flow time

Cell-3:

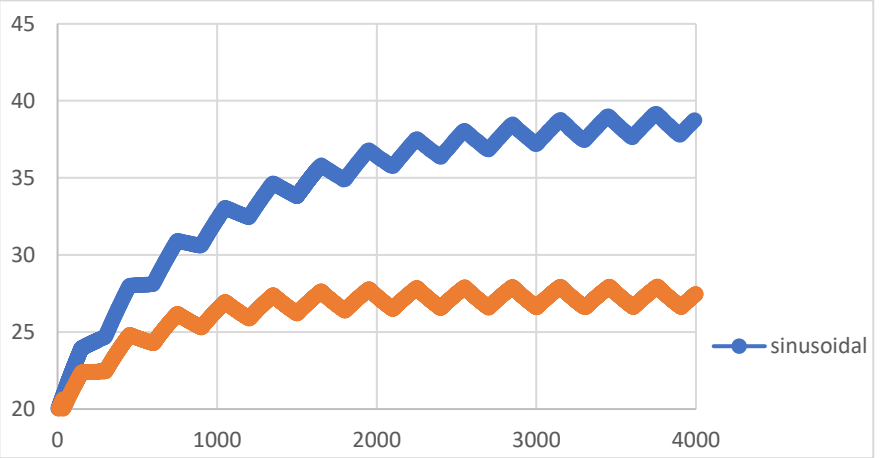

Fig-21: Comparison of two inlet BC for cell-3 Temperature variation vs flow time

Cell-4:

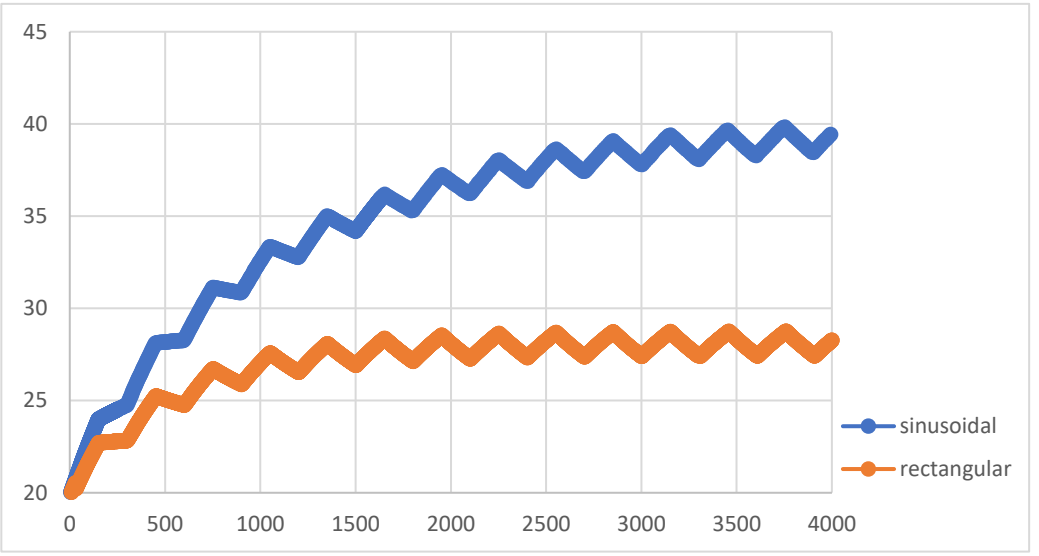

Fig-22: Comparison of two inlet BC for cell-4 Temperature variation vs flow time

Cell-5:

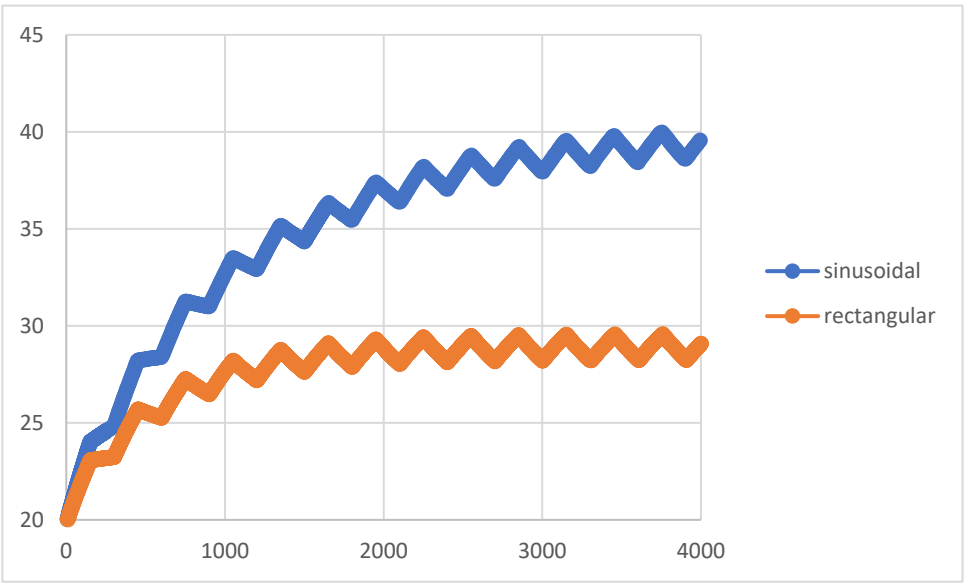

Fig-23: Comparison of two inlet BC for cell-5 Temperature variation vs flow time

Cell-6:

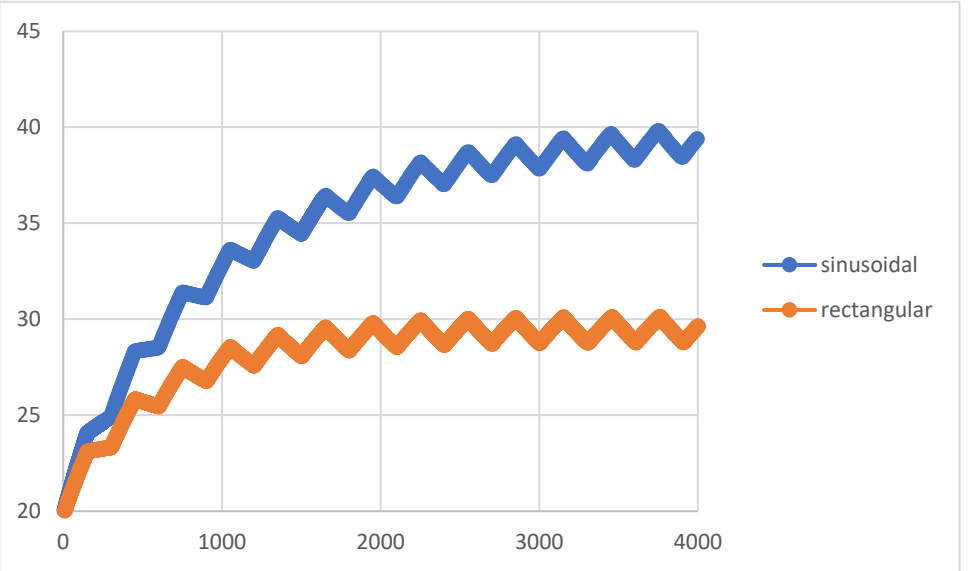

Fig-24: Comparison of two inlet BC for cell-6 Temperature variation vs flow time

Cell-7:

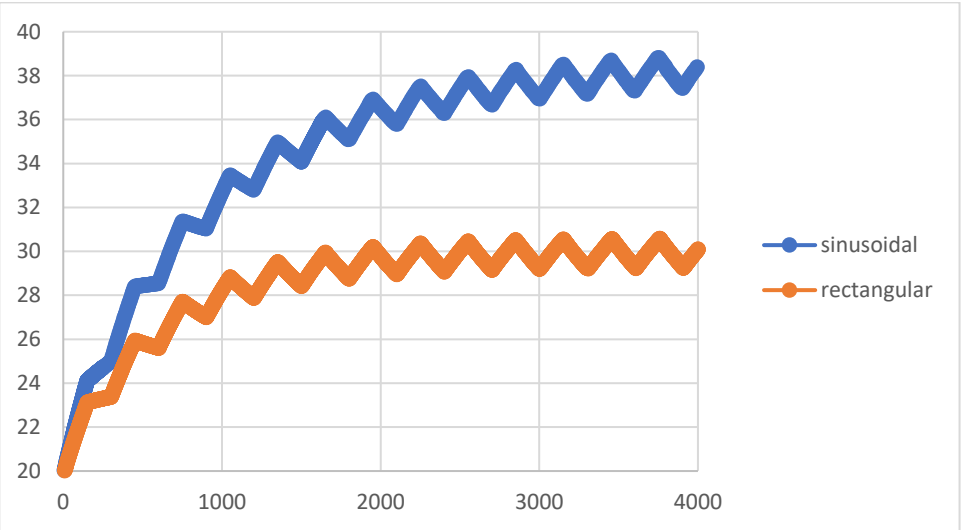

Fig-25: Comparison of two inlet BC for cell-7 Temperature variation vs flow time

Cell-8:

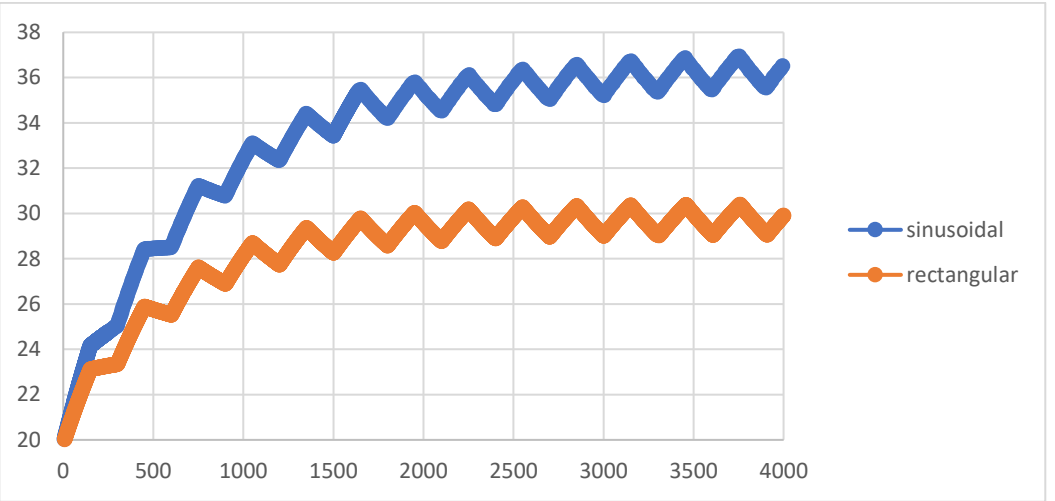

Fig-26: Comparison of two inlet BC for cell-8 Temperature variation vs flow time

Chapter-5

CONCLUSION

After referring several research papers related to battery pack thermal cooling using different methods, we came to understand that there was no such paper where sinusoidal inlet boundary condition is introduced for air cooling of lithium-ion battery pack. Firstly, we validated our results with one of the air-cooling papers using unidirectional flow case as discussed before. Then we successfully got our 2D CFD model of LIB pack after numerical analysis using **Ansys fluent** software. We used this model for our further study. After modifying the same model by using sinusoidal velocity profile instead of constant rectangular velocity, we generated some fruitful results such as temperature variations with flow time and with cell number as well. After this we compared our current results with last inlet boundary condition. We finally concluded some very important points out of this numerical analysis of LIB pack.

- In comparison plot, we can easily observe that temperature of sinusoidal inlet case is much higher than rectangular constant velocity condition.

- So even-though our aim or goal was to get better thermal cooling but we failed to achieve this as temperature was getting increased with flow time for inner cells.

- Although battery temperature did not exceed the operating temperature limit i.e.,40^0C but it was close to this in case of sinusoidal inlet condition. Maximum temperature difference came out to be 4.28^0C which is within the acceptable range. Whereas we were getting a maximum temperature of 29.5^0C and MTD as 5.36^0C, providing better cooling.

- It is concluded that we should not use sinusoidal inlet velocity condition with unidirectional air cooling as this has not provided any effective desired cooling.

- We can use our 2D LIB pack model with any other cooling methods as this model is much accurate.

References

1. Žukauskas, A. and Ulinskas, R., "Efficiency parameters for heat transfer in tube banks", *Heat Transfer Engineering*, volume *6*(1), pp.19-25, (1985)

2. Mahamud, R. and Park, C, "Reciprocating air flow for Li-ion battery thermal management to improve temperature uniformity", *Journal of Power Sources*, volume *196*(13), pp. 5685-5696, (2011)

3. M. H. Parekh, B. Li, M. Palanisamy, T. E. Adams, V. Tomar and V. G. Pol, "In Situ Thermal Runaway Detection in Lithium Ion Battery with an Integrated Internal Sensor", ACS Applied Energy Materials, volume 3, pp. 7997-8008, (2020).

4. T. Cai, A. G. Stefanopoulou and J. B. Siegel, "Early Detection for Thermal Runaway Based on Gas Sensing", The Electrochemical Society, volume 166 , pp. 2431-2443, (2019) .

5. J. Kim, J. Oh and H. Lee, "Review on Lithium-Ion Battery Thermal Management System for Electric Vehicle", Applied Thermal Engineering, volume 149, pp. 192-212, (2018).

6. J. E, M. Yue, J. Chen, H. Zhu, Y. Deng, Y. Zhu, F. Zhang, M. Wen, B. Zhang and K. Siyi, "Effects of the different air cooling strategies on cooling performance of a Lithium Ion Battery module with baffle", Applied Thermal Engineering, volume 144, pp. 231-241, (2018)

7. Bubbico, F. D'annibale, B. Mazzarotta and C. Menale, " Air Cooling of Lithium Ion Battery: an Experimental Analysis", Chemical Engineering Transactions, volume 57, pp. 379-384, (2017).

8. Y. Wang, & J Jiang, Y Chung , W. Chen and C. M. Shu, “Forced-air cooling system for large-scale lithium-ion battery modules during charge and discharge processes” , Journal of Thermal Analysis and Calorimetry, volume 135, pp. 2891–2901 ,(2018).

9. K. Chen, T. Han, B. Khalighi and P. Klaus. “Air Cooling Concepts for Li-Ion Battery Pack in Cell Level”, ASME 2017 Heat Transfer Summer Conference, pp. V001T09A00, (2017).

10. L. H. Saw, H. M. Poon, H. S. Thiam, Z. Cai, W. T. Chong, N. A. Pambudi, and Y. J. King, "Novel thermal management system using mist cooling for Lithium Ion Battery packs," Applied Energy, volume 223, pp. 146-158,(2018).

11. Z. An, C. Xing, L. Zhao, and Z. Gao, “Numerical investigation on integrated thermal management for a Lithium Ion Battery module with a composite phase change material and liquid cooling”. Applied Thermal Engineering, volume 163, pp. 114345, (2019).

12. M. Ramandi, I. Dincer, and G. Naterer, “Heat transfer and thermal management of electric vehicle batteries with phase change materials”. Heat and Mass Transfer, volume 47, pp. 777-788, (2011).

13. Z. Ling, F. Wang, X. Fang, X. Gao, and Z. Zhang, "A hybrid thermal management system for Lithium Ion batteries combining phase change materials with forced-air cooling," Applied Energy, volume 148, pp. 403-409, (2015).

14. J. Weng, D. Ouyang, X. Yang, M. Chen, G. Zhang, and J. Wang, “Optimization of the internal fin in a phase-change-material module for Lithium Ion Battery thermal management.” Applied Thermal Engineering. volume 167, pp. 114698 , (2019).

15. Y. Li, F. Qi, H. Guo, Z. Guo, G. Xu and J. Liu, Jiang. “Numerical investigation of Thermal runaway propagation in a Lithium Ion Battery module using the heat pipe

cooling system". Numerical Heat Transfer, Part A: Applications, volume 75, pp. 183-199, (2019).

16. T. Liu, Y. Liu , X. Wang, X. Kong and G. Li, "Cooling control of thermally-induced Thermal Runaway in 18,650 Lithium Ion Battery with water mist". Energy Conversion and Management, volume 199, pp. 116969, (2019).

17. J. Qin, S. Zhao, X. Liu and Y. Liu. " Simulation study on Thermal Runaway suppression of 18650 Lithium Ion Battery". Energy Sources, Part A: Recovery, Utilization, and Environmental Effects, volume 0, pp. 1-13, (2020).

18. T. Hatchard, D. MacNeil, A. Basu, and J. Dahn, "Thermal Model of Cylindrical and Prismatic Lithium Ion Cells", Journal of The Electrochemical Society , volume 148. pp. A755 , (2001).

19. G. Kim, A. Pesaran, and R. Spotnitz, "Three-Dimensional Thermal Abuse Model for Lithium Ion Cells", Journal of Power Sources, volume 170, pp. 476-489. (2007).

20. L.K., Yan, J., Chen, H., & Wang, Q.," Water cooling based strategy for lithium-ion battery pack dynamic cycling for thermal management system." Applied Thermal Engineering, 132, 575–585, (2018).

21. L.H. Saw, Y. Ye, A.A.O. Tay, W.T. Chong, S.H. Kuan, M.C. Yew, "Computational fluid dynamic and thermal analysis of Lithium-ion battery pack with air cooling," Appl. Energy. 177 (2016) 783–792.

22. E. Jiaqiang, D. Han, A. Qiu, H. Zhu, Y. Deng, J. Chen, X. Zhao, W. Zuo, H. Wang, J. Chen, Q. Peng, "Orthogonal experimental design of liquid-cooling structure on the

cooling effect of a liquid-cooled battery thermal management system, “Appl. Therm. Eng. 132 (2018) 508–520.

23. D. Zou, X. Ma, X. Liu, P. Zheng, Y. Hu, “Thermal performance enhancement of composite phase change materials (PCM) using graphene and carbon nanotubes as additives for the potential application in lithium-ion power battery”, Int. J. Heat Mass Transf. 120 (2018) 33–41.

24. R. Bubbico, F. D'annibale, B. Mazzarotta and C. Menale, “ Air Cooling of Lithium Ion Battery: an Experimental Analysis”, Chemical Engineering Transactions, volume 57, pp. 379-384, (2017).

25. K. Chen, T. Han, B. Khalighi and P. Klaus. “Air Cooling Concepts for Li-Ion Battery Pack in Cell Level”, ASME 2017 Heat Transfer Summer Conference, pp. V001T09A00, (2017).

26. L. H. Saw, H. M. Poon, H. S. Thiam, Z. Cai, W. T. Chong, N. A. Pambudi, and Y. J. King, "Novel thermal management system using mist cooling for Lithium Ion Battery packs," Applied Energy, volume 223, pp. 146-158,(2018).

27. Z. An, C. Xing, L. Zhao, and Z. Gao, “Numerical investigation on integrated thermal management for a Lithium Ion Battery module with a composite phase change material and liquid cooling”. Applied Thermal Engineering, volume 163, pp. 114345.